B68 11029

BELLCOMM, INC.
955 L'ENFANT PLAZA NORTH, S.W. WASHINGTON, D.C. 20024

SUBJECT: Spectrum Analysis of Apollo 4 and Apollo 6 Data - Case 320

DATE: November 12, 1968

FROM: J. Z. Menard

ABSTRACT

Continuous spectrum analysis displays of a number of Apollo 4 (AS-501) and Apollo 6 (AS-502) flight telemetry signals have been made at Bell Telephone Laboratories, Inc., to explore the usefulness of this technique for diagnosis of the unexpectedly large low-frequency longitudinal oscillation (POGO) experienced on the Apollo 6 flight. This memorandum describes the technique, and presents results from analysis of a selected set of Apollo 4 and Apollo 6 measurements. The more interesting indications from these raw data are:

1. Evidence of 5-6 hertz (POGO) in the thrust chamber pressure spectra of all engines of Apollo 6, but not in Apollo 4.

2. Indication of substantially similar dynamic responses in the gimbal block acceleration spectra of Apollo 4 and Apollo 6, with almost identical frequency-time histories in the 5-6 hertz (POGO) region.

3. An anomalous indication in the thrust chamber pressure and gimbal block vibration spectra of the Number 5 engine of Apollo 6 at about T+120 seconds.

4. Indication of a prominent (structural?) resonance in the 18-20 hertz region in the gimbal block spectra of both Apollo 4 and Apollo 6.

5. Indications of very similar dynamic response histories in the payloads of Apollo 4 and Apollo 6, with evidence that in the 4-7 hertz region, a descending-frequency component seen in the LTA came into coincidence with an ascending-frequency component in the CSM at the time POGO occurred.

6. An indication that on Apollo 6, the LTA Y-axis experienced a change in coupling to the vehicle at about T+130 seconds while the Z-axis does not evidence a corresponding change.

BELLCOMM, INC.
955 L'ENFANT PLAZA NORTH, S.W. WASHINGTON, D. C. 20024

SUBJECT: Spectrum Analysis of Apollo 4 and Apollo 6 Data - Case 320

DATE: November 12, 1968

FROM: J. Z. Menard

MEMORANDUM FOR FILE

1.0 INTRODUCTION

A number of Apollo 4 and Apollo 6 flight measurement signals have been processed using a real-time spectrum analysis and display technique which was developed at Bell Telephone Laboratories as an extension of "visible speech" research and has been found to be a powerful aid in the diagnosis of complex dynamic processes, such as the behavior of vibrating systems. The essential characteristics of the technique are:

(a) Repetitive measurements of the short-term spectrum of the input signal.

(b) Display of the repetitive series of spectrum measurements as a time-frequency-density plot to provide a time history of the spectrum, in which the frequency, bandwidth, and relative magnitudes of the constituent components can be seen.

(c) Optimization of the bandwidth and time window length used for the spectrum measurements to accommodate the dynamic characteristics of the input signal.

In principle, the repetitive measurements of the short-term spectrum can be made by several approaches which involve different implementation but are functionally equivalent for this use:

(a) A bank of narrowband filters with sequentially commutated outputs.

(b) A digital store, with repetitive high-speed non-destructive readout, followed by a heterodyne swept-filter analyzer.

(c) A fast Fourier Transform (FFT) analyzer.

The time-frequency-density plot can also be generated by several methods:

(a) Using a continuous advance film camera to photograph an oscilloscope which has the X-axis synchronized to the analysis sweep, and the Z-axis intensity modulated by the spectrum level.

(b) Using a facsimile recorder synchronized to the analysis sweep, and modulated by the spectrum level.

Figure 1 illustrates the stored memory-heterodyne analyzer implementation with output options including the facsimile recorder, and notes typical parameters which might be used for analysis and display of flight data. All of the implementations are capable of operating in real time, and can provide the time-frequency-density displays and conventional power spectrum density X-Y plots at a fraction of the equipment and operating cost of obtaining PSD plots alone through use of a general purpose computer.

The time-frequency-density display of such equipment provides a time history of the input spectrum which facilitates recognition of:

(a) frequency-related components in a signal input,

(b) time-related characteristics in a signal input,

(c) correlated characteristics present in different signal inputs.

This type of display has proven useful in the diagnosis of complex phenomena, where it quickly makes apparent relations and events which can then be explored by more quantitative but less easily interpreted power spectrum density measurements at selected time intervals.

2.0 ANALYSIS RESULTS

Selected flight telemetry signals from Apollo 4 and Apollo 6 were processed at Bell Telephone Laboratories using equipment which was designed for a different application. Some improvisation was required to process the flight data, and while the results clearly demonstrate the potential of the technique, it is probable that improvements can be made by optimizing the analysis bandwidth, the time window length, and the input/output transfer characteristic of the system. In particular, the equipment used at Bell Telephone Laboratories employs an automatic gain control designed to normalize the average spectrum across the frequency and time dimensions, and this necessitates caution in interpreting relative spectrum levels at points which are widely separated in time or frequency. For interpretation of flight data, a system with fixed gain and perhaps a log (dB) output transfer function to the display appears desirable.

The results which follow represent the analysis of data obtained from the Marshall Space Flight Center and the Manned Spacecraft Center in the form of dubbed tape recordings of the flight telemetry data. As the transducers and telemetry system can introduce spurious components in the data, caution is required in interpretation of the results. Consequently, in discussing the results which follow, attention will be limited to prominent spectrum features which definitely appear to be flight related because of their dynamic behavior, or their appearance in several independent measurements. It should be emphasized that these results are raw data, subject to screening for validity and significance.

2.1 LAUNCH VEHICLE DATA

2.1.1 Thrust Chamber Pressure

Figure 2 shows the spectrum of the thrust chamber pressure signal from engine #5 (the center engine) of the S-IC stage of Apollo 6 from liftoff to cutoff. This measurement was designed and scaled to record the steady-state thrust pressure level, which is about 1100 pounds per square inch, and the analysis is looking at the fluctuation component on this signal, which is in the range of 20 psia peak to peak, or more than 30 decibels below the normal deviation of the telemetry channel. At this level, spurious signals from electrical noise are quite possible and attention is therefore directed only to the following prominent features of the spectrum:

2A. A component in the 0-2 hertz region throughout the flight.

2B. A component at ≈5 hertz between 110-140 seconds (POGO).

2C. A broad spectrum peak (partially suppressed by automatic gain control) around 25 hertz at liftoff, and dropping to about 22 hertz during the flight.

2D. A prominent component at about 40 hertz, unstable in frequency, which decreases in bandwidth during flight, and appears to make a step frequency shift to 35 hertz at about 120 seconds.

Figure 3 shows the entire set of these measurements for the five engines of Apollo 4 and Apollo 6. Note that:

3A. The 0-2 hertz energy appears in similar fashion on all engines of both flights.

3B. There is no evidence of systematic energy in the 5 hertz region on Apollo 4, but it is seen on all engines of Apollo 6 during the 120-140 second period.

3C. There is a prominent spectral peak in the 30-35 hertz region on all control engines of both flights. However, there are engine-to-engine differences in the character of the components, with Apollo 6 showing a systematic tendency to be more prominent, somewhat higher in frequency, less stable, and to decrease in frequency during flight.

3D. The center engines (#5) on Apollo 4 and Apollo 6 show components in the 35-40 hertz region, but on Apollo 6 this component is more prominent and exhibits the unique discontinuity at about 120 seconds, as mentioned under 2D above.

3E. All engines of Apollo 4 show a prominent component at about 50 hertz at liftoff, rising to about 60 hertz at 70 seconds. Similar, but less stable components are evident in some of the engines of Apollo 6.

<u>2.1.2 Gimbal Block Vibration</u>

Figure 4 shows the spectrum of the #5 engine gimbal block vibration on Apollo 6. Features of interest are:

4A. A component at ≈4 hertz in the 5-15 second time period, which can be interpolated to reappear prominently, with an upward frequency shift, in the 100-145 second period (POGO).

4B. Prominent energy in the 16-20 hertz region throughout the flight, exhibiting an upward trend in the 0-65 second time period, then shifting downward and repeating the upward trend. This feature was not seen in the thrust chamber pressure spectrum, and may indicate a structural resonance.

4C. A prominent component in the 38-40 hertz region, of narrow bandwidth, which in the early part of the flight does not correlate in detail with the similar component seen in the thrust chamber pressure spectrum of that engine, but does correlate closely toward the end, and exhibits exactly the same step shift in frequency at about 120 seconds. It may be conjectured that this indicates a structural resonance excited by the composite energy of the five engines in this band.

4D. A component at about 50 hertz at liftoff, rising to about 60 hertz at 70 seconds, and correlating closely with 3E in the thrust chamber pressure spectra.

Figure 5 shows for comparison the gimbal block vibration signatures of Apollo 4 and Apollo 6, analyzed over the frequency range of 0 to 50 hertz and displayed with a compressed time dimension which increases the slope of frequency shifts and thus facilitates recognition of time-varying features.

The lower display of Figure 5 is the same Apollo 6 gimbal block signal as was seen in Figure 4, and despite the difference in appearance, inspection will confirm that they show the same spectrum features. The center display of Figure 5 is the corresponding gimbal block vibration spectrum from Apollo 4, and the upper display is the spectrum from the engine #1 gimbal block of Apollo 4. Its counterpart on Apollo 6 was defective. The principal features seen in comparison of these measurements are:

5A. In the 5-6 hertz region, the gimbal block vibration spectra of Apollo 4 and Apollo 6 were remarkably alike during the "POGO" time period, and a similar component was seen in the Apollo 4 measurements during the early part of the flight.

5B. Apollo 4 and Apollo 6 showed very similar behavior in the 16-18 hertz region.

5C. In the 35-40 hertz region, Apollo 4 and Apollo 6 showed similar spectral components, but only Apollo 6 exhibited the step discontinuity at 120 seconds.

2.1.3 S-IC-6 Static Firing

Figure 6 through Figure 10 show for each of the engines of S-IC-6 the spectra of the fuel pump inlet pressure, LOX pump inlet pressure, and thrust chamber pressure during the static firing of that stage. The principal indications from this set of measurements are:

A. There are significant engine-to-engine differences.

B. Major components are seen at ≈12 hertz (engines 1, 3 and 5) 30-35 hertz (strong on engines 2 and 4, weak on 1 and 3).

C. The frequency stability and bandwidth of the 30-35 hertz components on engines 2 and 4 are similar in character to those seen in the Apollo 4 and Apollo 6 thrust chamber pressure spectra.

D. There is high correlation between the spectra of the thrust chamber pressure, fuel and LOX inlet pressures.

2.2 SPACECRAFT DATA

Figure 11 is the spectrum of the Y-axis* tower acceleration on Apollo 6. Prominent features are:

11A. A 2-3 hertz lateral oscillation throughout the entire flight.

11B. A 5-6 hertz "POGO" during the 110-130 second time period.

11C. Broadband energy in the 8-15 hertz region through the early part of the flight.

11D. Broadband energy in the 35 hertz region from liftoff to about T+110 seconds. This is loosely correlated with energy seen in the thrust chamber pressure and gimbal block spectra, and could indicate propagation of this energy through the vehicle.

Figure 12 is the spectrum of the Z-axis* acceleration at the command module on Apollo 6. Prominent features are:

12A. 2-3 hertz energy, periodically varying in level through the flight.

12B. 5-6 hertz energy, periodically varying in level, and drifting downward in frequency throughout the flight.

---

*In all measurements, the axis notations are: X=longitudinal, Y=yaw, Z=pitch.

12C. 5-6 hertz energy appearing at ≈T+108 seconds, and ending at ≈T+140 seconds, with a distinct upward frequency shift during this period, such that it is coincident with 12B at about T+125 seconds.

12D. ≈16 hertz energy, varying in level, at times during the flight.

12E. Broadband energy in the 22-25 hertz region from liftoff to about T+70 seconds.

12F. Narrowband frequency-stable energy at ≈44 hertz from liftoff to about T+30 seconds.

12G. Narrowband frequency-stable energy at ≈62 hertz from liftoff to about T+40 seconds.

The frequency stability of 12F and 12G leads to the suspicion that they may not be vibration components.

Figure 13 is the spectrum of the axial acceleration on the command module sway brace in Apollo 6. Prominent features are:

13A. A 5-6 hertz component (suppressed by automatic gain control in the 35 to 75 second time period) which increases in frequency during flight, and exhibits many harmonics, with emphasis on the odd series, in the 100 to 130 second time period. The fundamental 5-6 hertz component continues to the end of the burn, but abrupt changes are seen in the harmonic series at about 128 seconds, and at ≈134 seconds, indicating large changes in the wave form of this spectral component at those times.

13B. An unstable component at about 10 hertz during the first 30 seconds of flight.

13C&D. Broad bands of energy at about 25 and 35 hertz from liftoff to about T+100 seconds.

Figure 14 is the spectrum of the axial acceleration on the command module sway brace on Apollo 4 and is directly comparable with Figure 13, the corresponding measurement on Apollo 6. The prominent features A, B, C and D of this measurement on Apollo 4 are essentially identical with those of Apollo 6, with the exception that on Apollo 4, a lower number of harmonics of the 5-6 hertz component were seen, and the broad bands of energy, C and D, were slightly higher in frequency on

Apollo 4 than on Apollo 6. The similarity of the dynamic behavior of these command module measurements on the two flights is striking.

Figure 15 is the spectrum of the Y-axis acceleration of LTA-2R on Apollo 6. The principal features are:

15A. A 5-6 hertz component which periodically varies in level during the flight, and during the 100-130 second time period, increases in level and shows a number of harmonics. Note that this component is not evident after about T+130 seconds.

15B. Some ≈12 hertz energy in the 10-20 second time period.

15C. A broad band of energy around 30 hertz, most evident in the 50-100 second time period.

15D. Some energy at ≈58 hertz at liftoff, reappearing at decreasing level, and increasing in frequency in the first half of the flight.

Figure 16 is the spectrum of the Z-axis acceleration of LTA-2R on Apollo 6. The prominent features are:

16A. ≈2-1/2 hertz energy in the 90-115 second time period.

16B. A 5-6 hertz component which is evident throughout the flight, with a progressive downward shift in frequency, and in the 110-135 second time period is apparently crossed by a component with an upward frequency shift. It is interesting to note that this component in the LTA-2R is decreasing in frequency during the flight, while command module component 13A is increasing in frequency, and these appear to coincide in frequency at about T+125 seconds, which corresponds to the maximum "POGO" on the Apollo 6 flight.

Figures 17 and 18 are the spectra of a set of corresponding LTA measurements on Apollo 4 and Apollo 6, displayed with compressed time scales to facilitate comparisons. In the 5-7 hertz region, these show clearly the presence of two components - one increasing in frequency, and the other decreasing, in both Apollo 4 and Apollo 6. Harmonics appear at the time these components coincide in frequency, and in all the expanded time scale displays this was seen to correspond to the period of maximum level. Careful comparison shows the upward-shifting components on Apollo 4 and Apollo 6 to be substantially identical but the downward-shifting component to be about one hertz higher in frequency on Apollo 6 than on Apollo 4. The significance of this difference is not known, but may warrant investigation, as it suggests differences in payload dynamics which may relate to POGO.

Figure 19 shows the spectra of several spacecraft measurements from Apollo 6, using the compressed time scale. The principal features are:

19A. 2-1/2 hertz energy is seen throughout the flight on the Y-axis and Z-axis of the tower.

19B. The 5-6 hertz "POGO" component is evident in all measurements.

19C. Broadband energy at ≈8 hertz is evident on the tower.

19D. Prominent components are seen on the tower in the 30-35 hertz region from liftoff to about T+100 seconds, and these are similar in character to components seen in the launch vehicle thrust chamber pressure spectra in this frequency region.

3.0 SUMMARY

The results obtained from continuous spectrum analysis of the selected flight measurements of Apollo 4 and Apollo 6 illustrate the use of this technique to portray the time history of a dynamic process, and provide some interesting but unevaluated indications of Apollo 4 and Apollo 6 performance. The indications of principal interest are:

(a) The thrust chamber pressure spectra showed the 5-6 hertz (POGO) component in Apollo 6, but not in Apollo 4. Both Apollo 4 and Apollo 6 had prominent 35-40 hertz components on all engines.

(b) The gimbal block vibration spectra showed Apollo 4 and Apollo 6 to have very similar dynamic behavior in the 5-6 hertz (POGO) region, in the 16-20 hertz region, and in the 35-40 hertz region. The 16-20 hertz component in the gimbal block spectra was not evident in thrust chamber pressure.

(c) The S-IC-6 static firing data show the fuel, LOX, and thrust chamber pressure spectra to be highly correlated. No energy peaks were found in the 5-6 hertz (POGO) region, but this may not be surprising, as the stage is restrained in the firing. Major components were seen in the 12 hertz and 30-35 hertz region, and the latter components resembled those seen in the Apollo 4 and Apollo 6 flight measurements.

(d) The most striking anomalous indication was the step discontinuity in the thrust chamber pressure and gimbal block spectra of engine #5 of Apollo 6 at about T+120 seconds. (This has been called to the attention of Boeing, who substantiated it by conventional power spectrum density plots covering that time period.)

(e) In the payload measurements of Apollo 4 and Apollo 6, generally similar time histories of dynamic response were seen. In both flights, in the 5-7 hertz region, a descending-frequency component was prominent in the LTA, and an ascending-frequency component was prominent in the command module. The descending-frequency component was slightly higher in frequency on Apollo 6 than on Apollo 4. The time of maximum "POGO" on Apollo 6 corresponds to the time of frequency coincidence of these components.

(f) On Apollo 6, the 5-6 hertz component is evident in the LTA Z-axis spectrum throughout the flight, but on the LTA Y-axis it ceases to be apparent at about the time of the 134 second event, suggesting a marked change in Y-axis coupling to the vehicle at that time.

The preliminary results of this work have been presented to representatives of MSFC and MSC to permit their assessment of the usefulness of the technique. If the indications from the present work appear promising, additional data from Apollo 4, Apollo 6, and from selected static firings and tests appear to be candidates for analysis. The Centers could, if desired, quickly establish an in-house capability to do this on a continuing basis, by making use of an assembly of commercially available signal processors and display devices. We have offered to provide assistance to them in the definition and assembly of a suitable system if desired.

4.0 ACKNOWLEDGMENT

The data presented in this memorandum were generated at Bell Telephone Laboratories. Especial appreciation is expressed for the support provided by members of the Ocean Systems Laboratory, the Military Digital Systems Laboratory, and the Reliability Engineering Center, for the interest and personal time they devoted to reduce telemetry data, prepare software programs, and modify and operate the analysis equipment which produced the spectrum analysis displays.

J. Z. Menard

203-JZM-sk

J. Z. Menard

Attachments
Figures 1-19

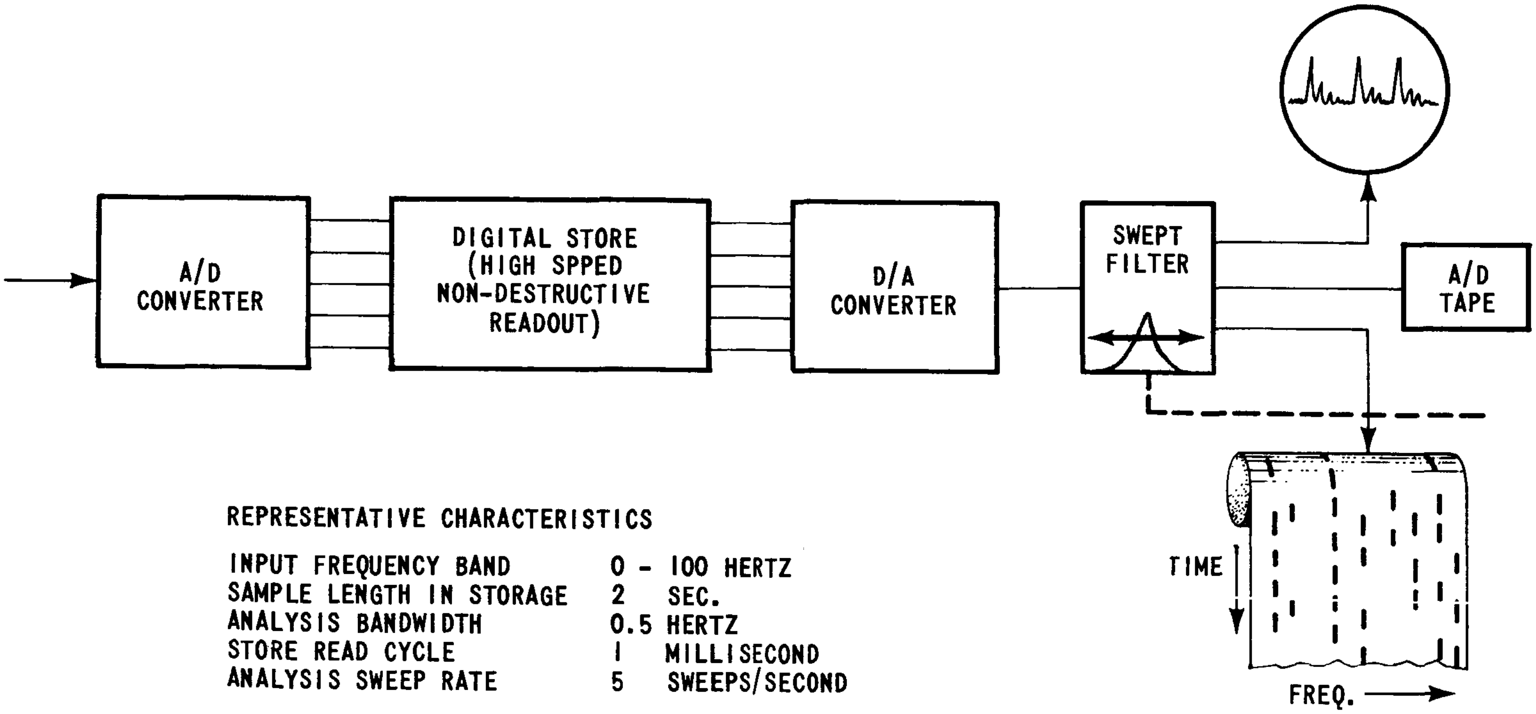

REPRESENTATIVE CHARACTERISTICS

INPUT FREQUENCY BAND	0 - 100 HERTZ
SAMPLE LENGTH IN STORAGE	2 SEC.
ANALYSIS BANDWIDTH	0.5 HERTZ
STORE READ CYCLE	1 MILLISECOND
ANALYSIS SWEEP RATE	5 SWEEPS/SECOND

SWEPT FILTER PSD IMPLEMENTATION

FIGURE 1

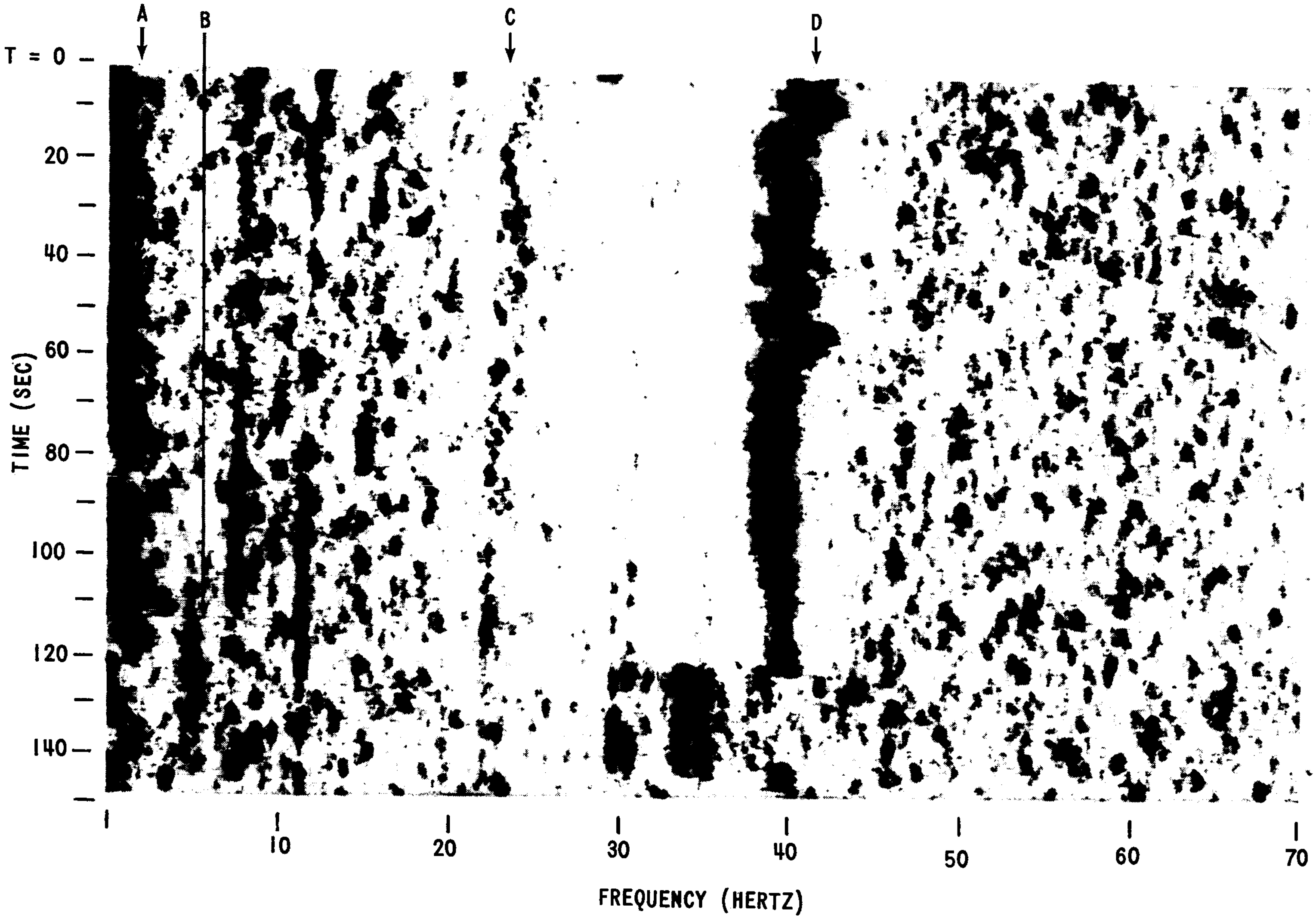

THRUST CHAMBER PRESSURE AS-502 (ENGINE #5)

FIGURE 2

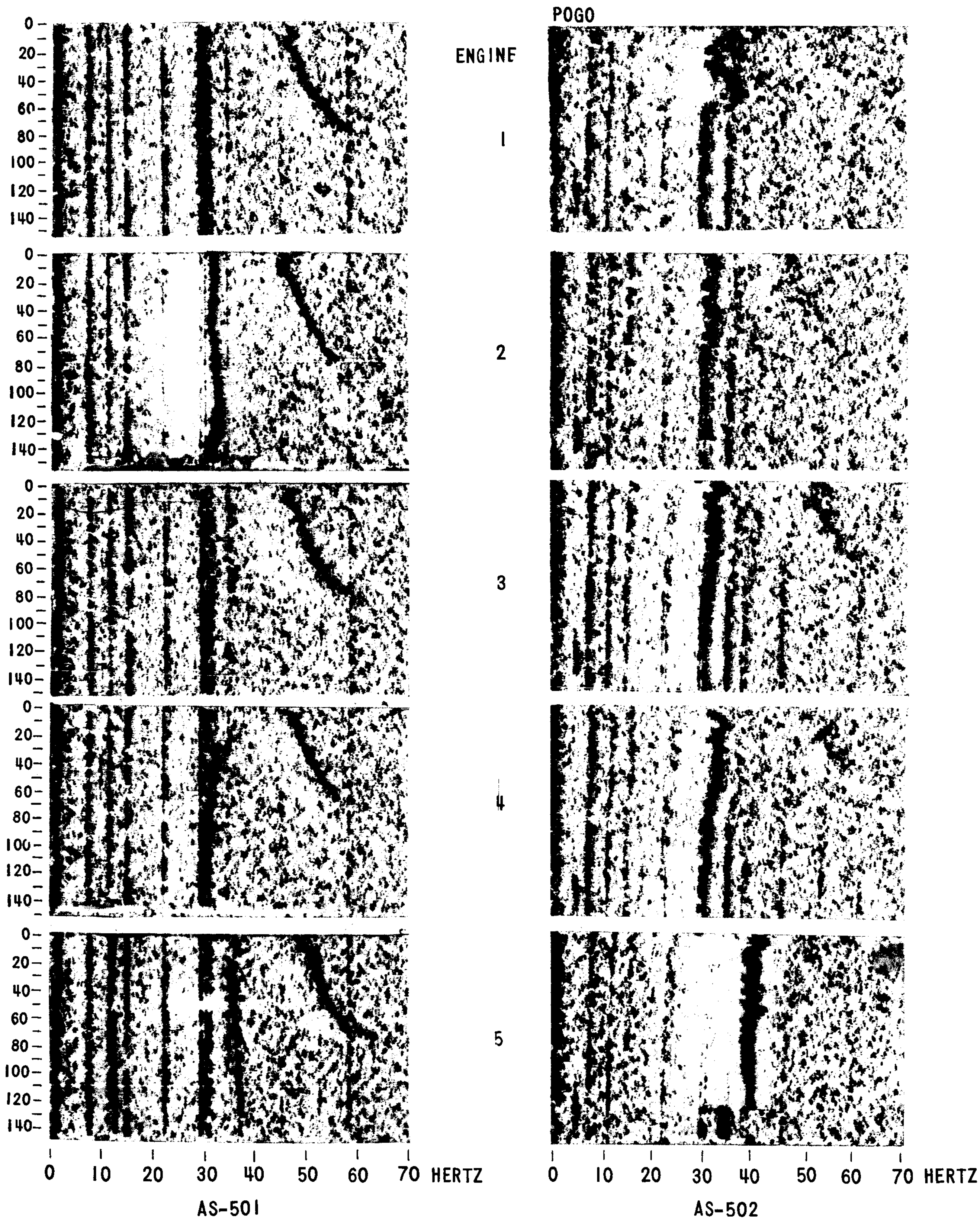

THRUST CHAMBER PRESSURE SPECTRA

FIGURE 3

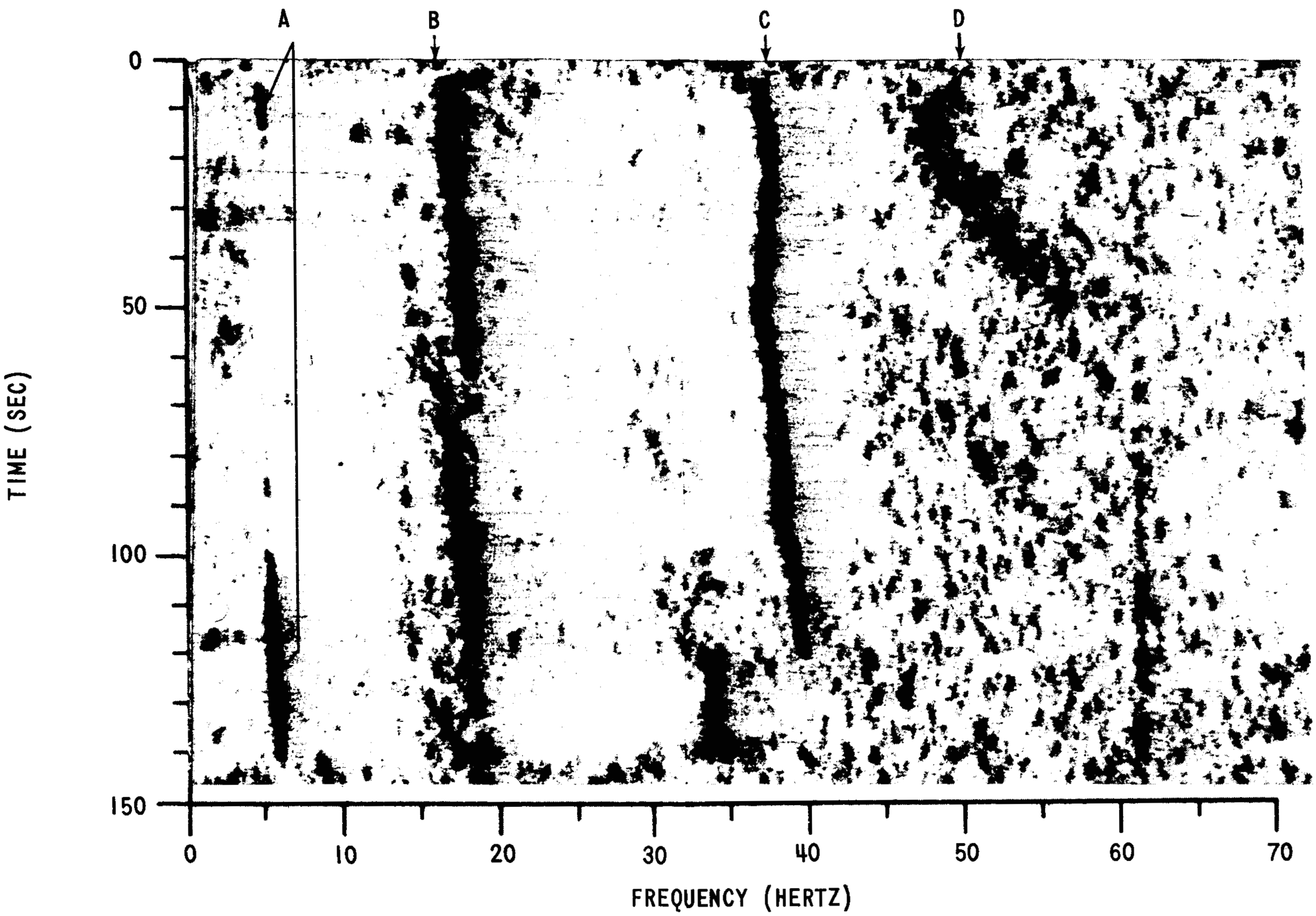

MEASUREMENT E83015 AS-502 GIMBAL BLOCK VIBRATION

FIGURE 4

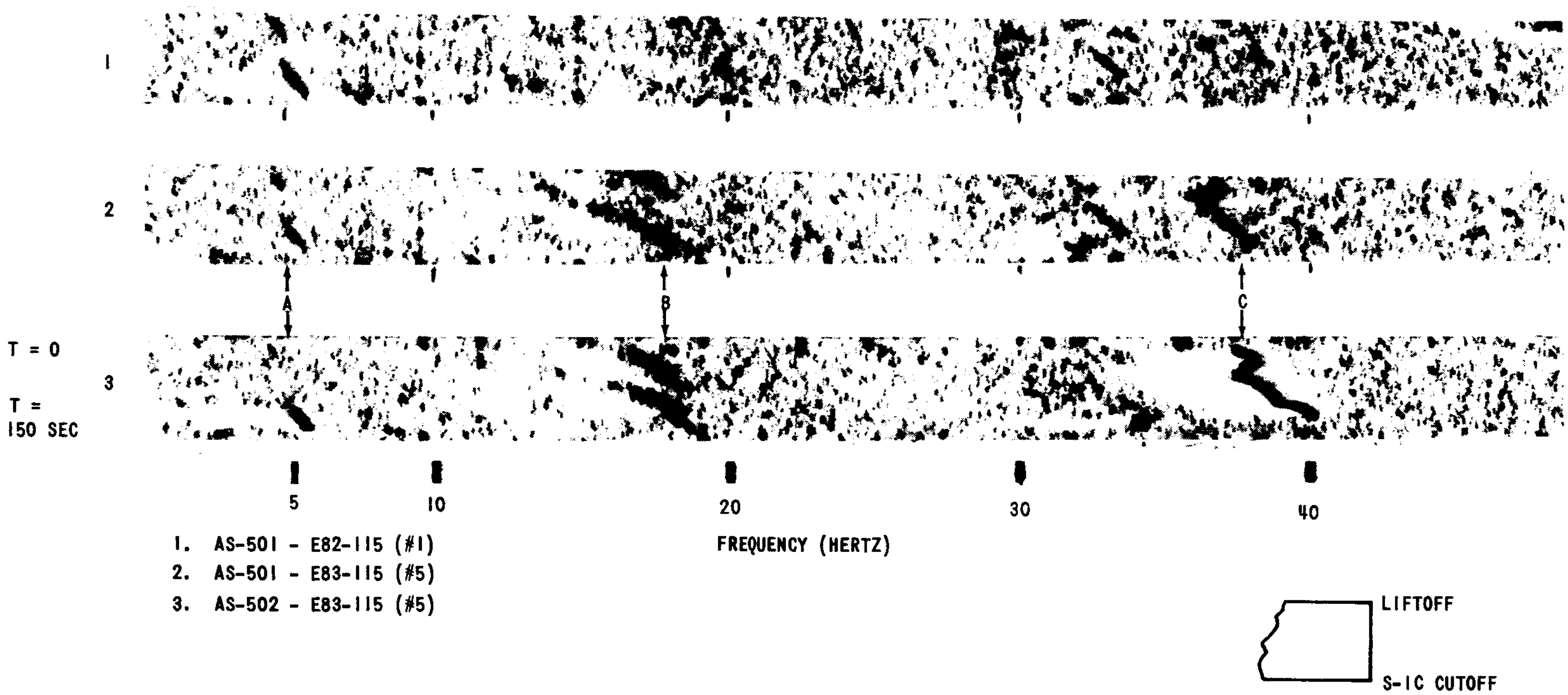

LONGITUDINAL VIBRATION S-IC GIMBAL BLOCK

FIGURE 5

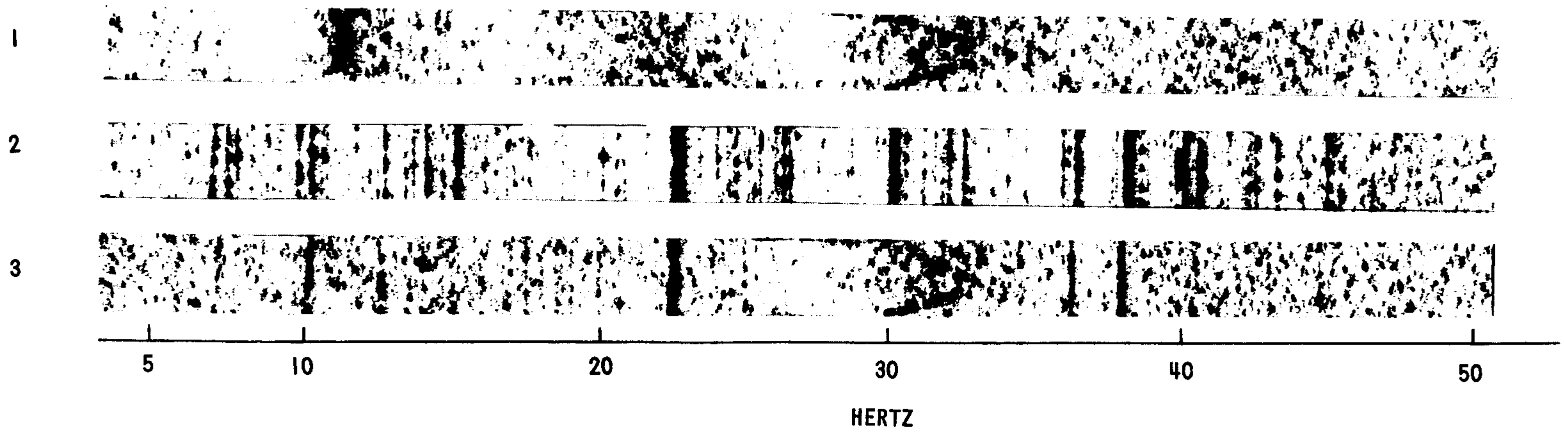

1 - DA1 FUEL PUMP #1 INLET PRESSURE
2 - DA2010 LOX PUMP INLET PRESSURE (DEFECTIVE)
3 - DA7 THRUST CHAMBER PRESSURE

ENGINE #1

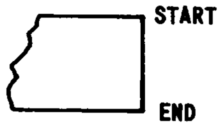

SPECTRUM ANALYSES - S-IC-6 STATIC FIRING

FIGURE 6

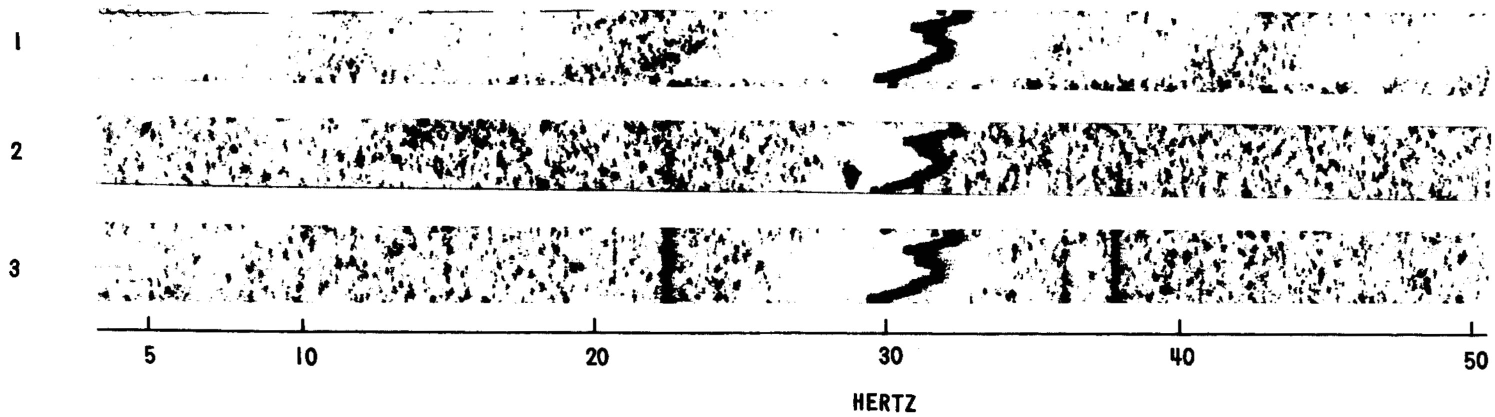

1 - DA1 FUEL PUMP #1 INLET PRESSURE
2 - DA2010 LOX PUMP INLET PRESSURE
3 - DA7 THRUST CHAMBER PRESSURE

ENGINE #2

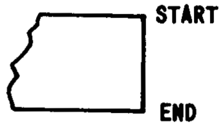

SPECTRUM ANALYSES - S-IC-6 STATIC FIRING

FIGURE 7

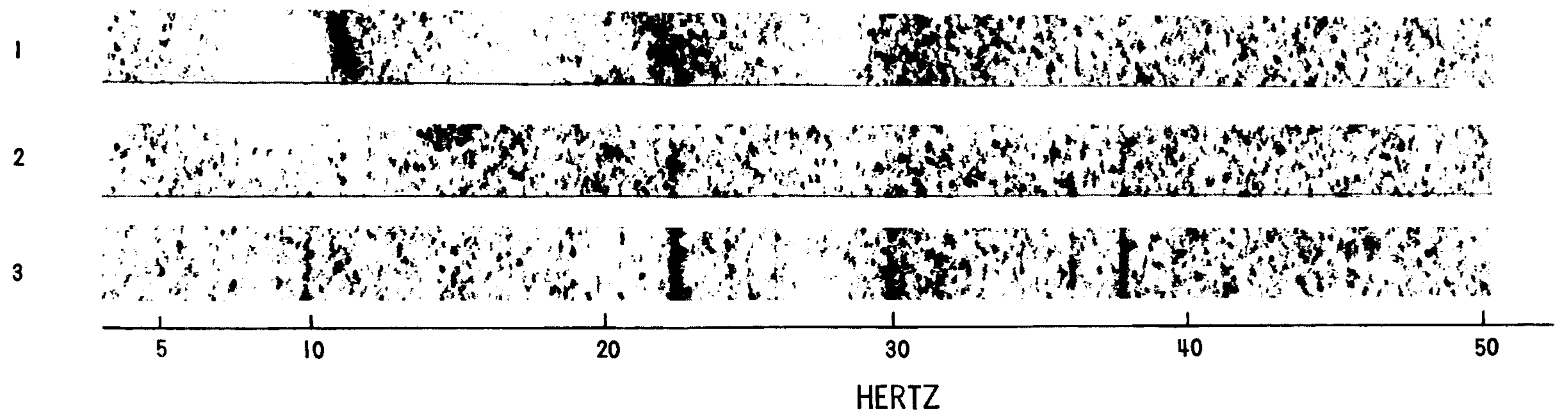

1 - DA1 FUEL PUMP #1 INLET PRESSURE
2 - DA2010 LOX PUMP INLET PRESSURE
3 - DA7 THRUST CHAMBER PRESSURE

ENGINE #3

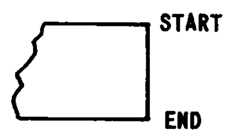

SPECTRUM ANALYSES - S-IC-6 STATIC FIRING

FIGURE 8

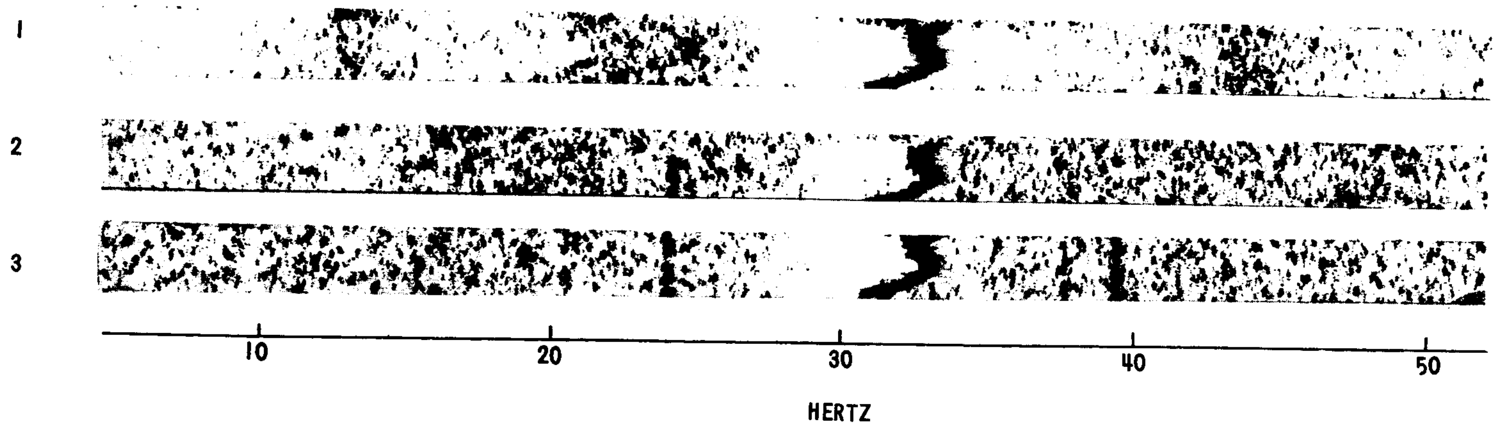

1 - DA1 FUEL PUMP #1 INLET PRESSURE
2 - DA2010 LOX PUMP INLET PRESSURE
3 - DA7 THRUST CHAMBER PRESSURE

ENGINE #4

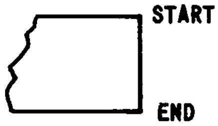

SPECTRUM ANALYSES - S-IC-6 STATIC FIRING

FIGURE 9

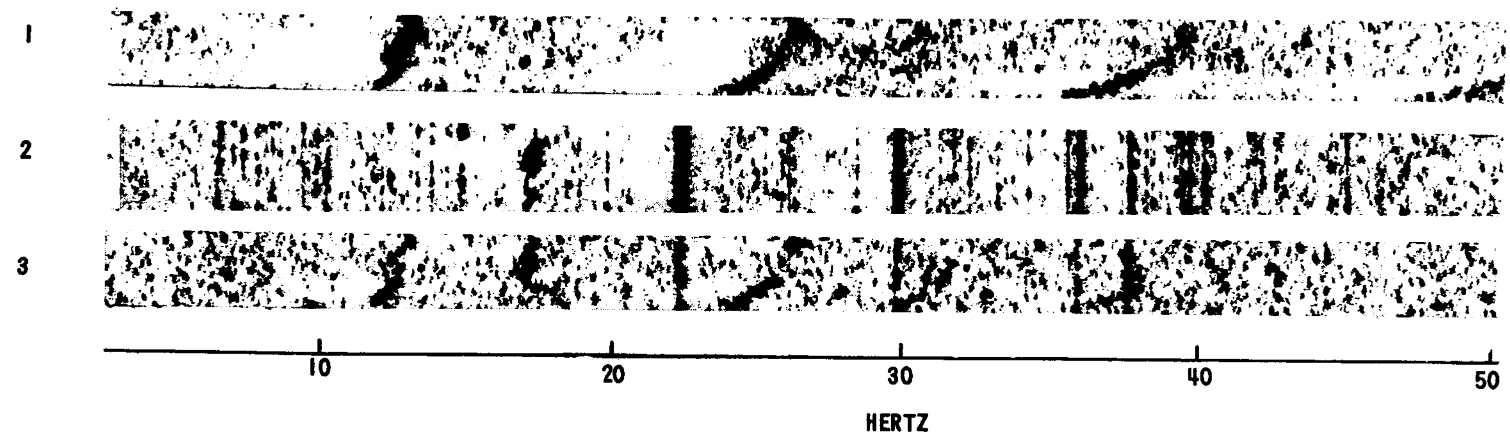

I - DA1 FUEL PUMP #1 INLET PRESSURE
2 - DA2010 LOX PUMP INLET PRESSURE (DEFECTIVE)
3 - DA7 THRUST CHAMBER PRESSURE

ENGINE #5

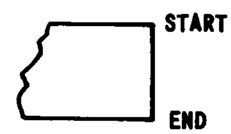

SPECTRUM ANALYSES - S-IC-6 STATIC FIRING

FIGURE 10

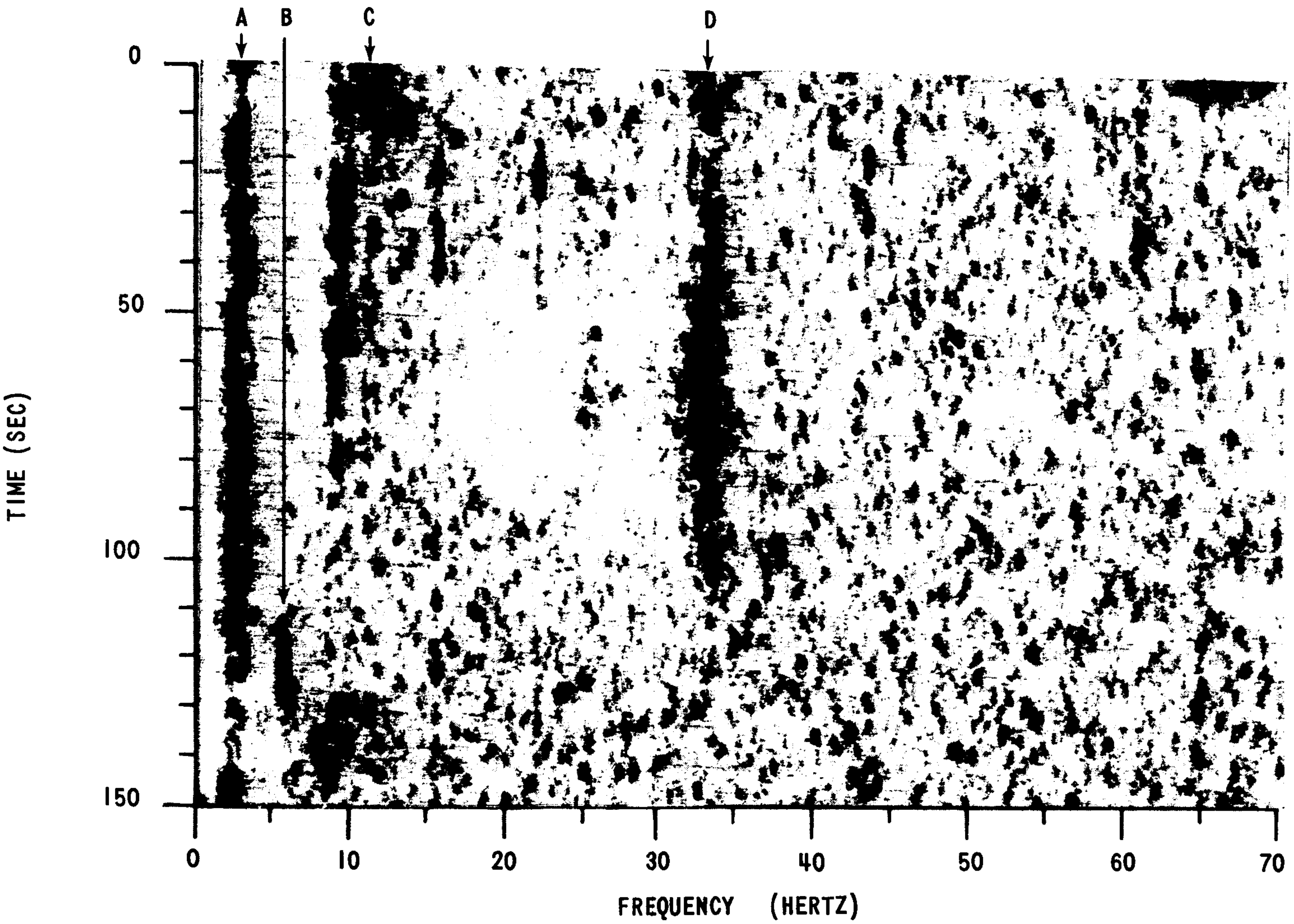

MEASUREMENT LA 0011A AS-502 Y AXIS TOWER ACCELERATION

FIGURE 11

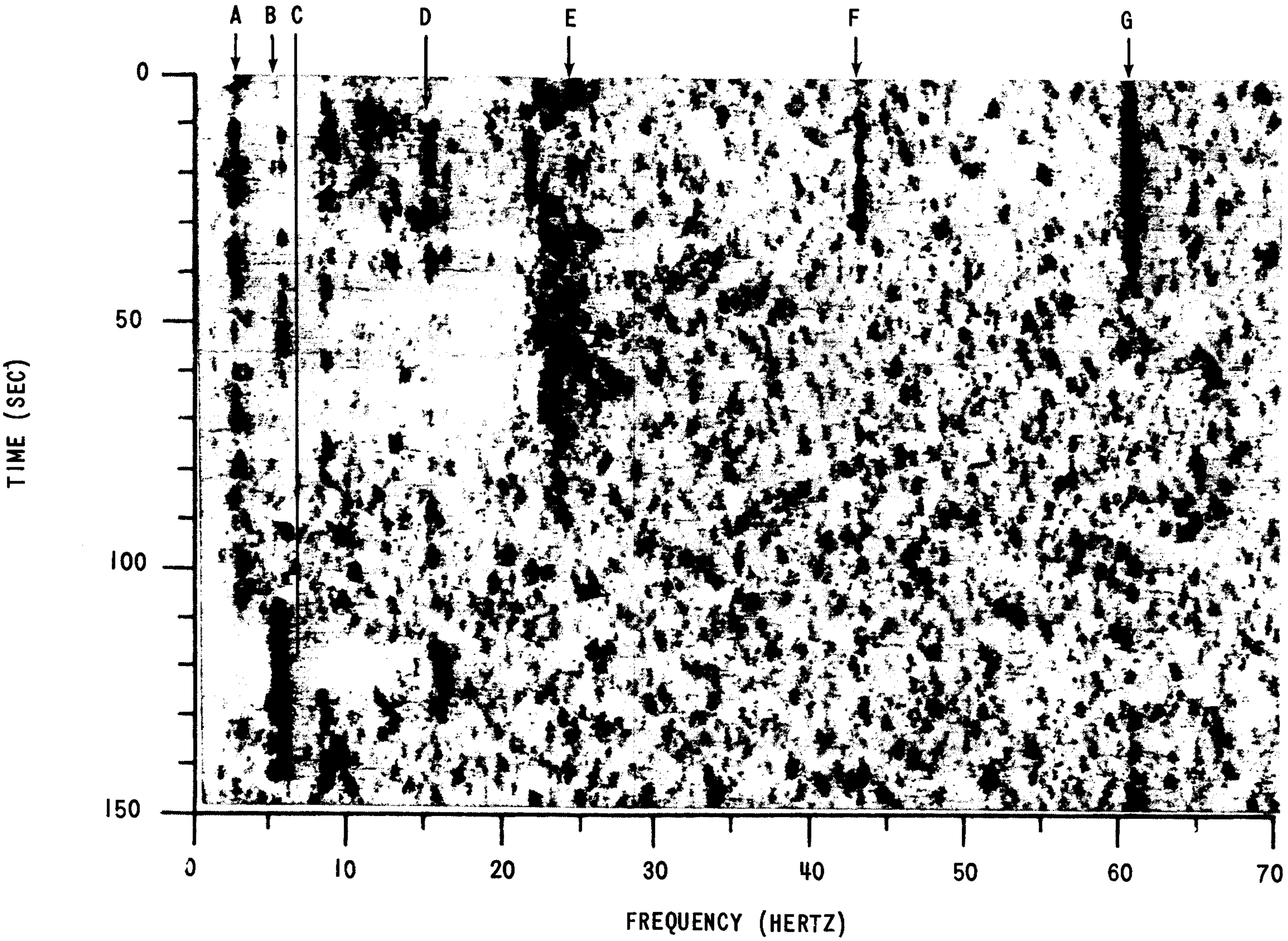

MEASUREMENT CA 0007A AS-502 Z AXIS ACCELERATION - S/C 020

FIGURE 12

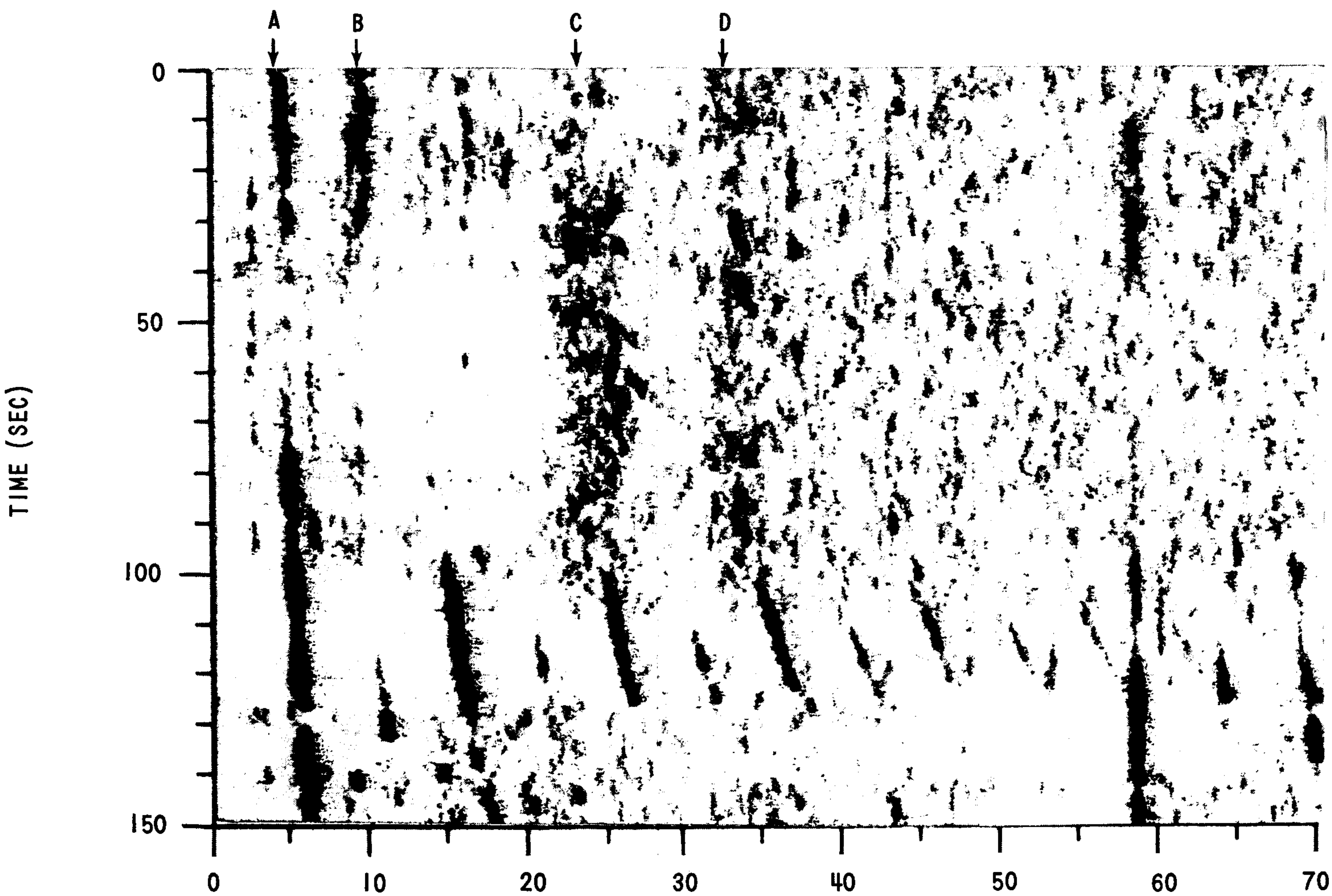

MEASUREMENT CK 0038A AS-502 AXIAL ACCELERATION - CM SWAY BRACE

FIGURE 13

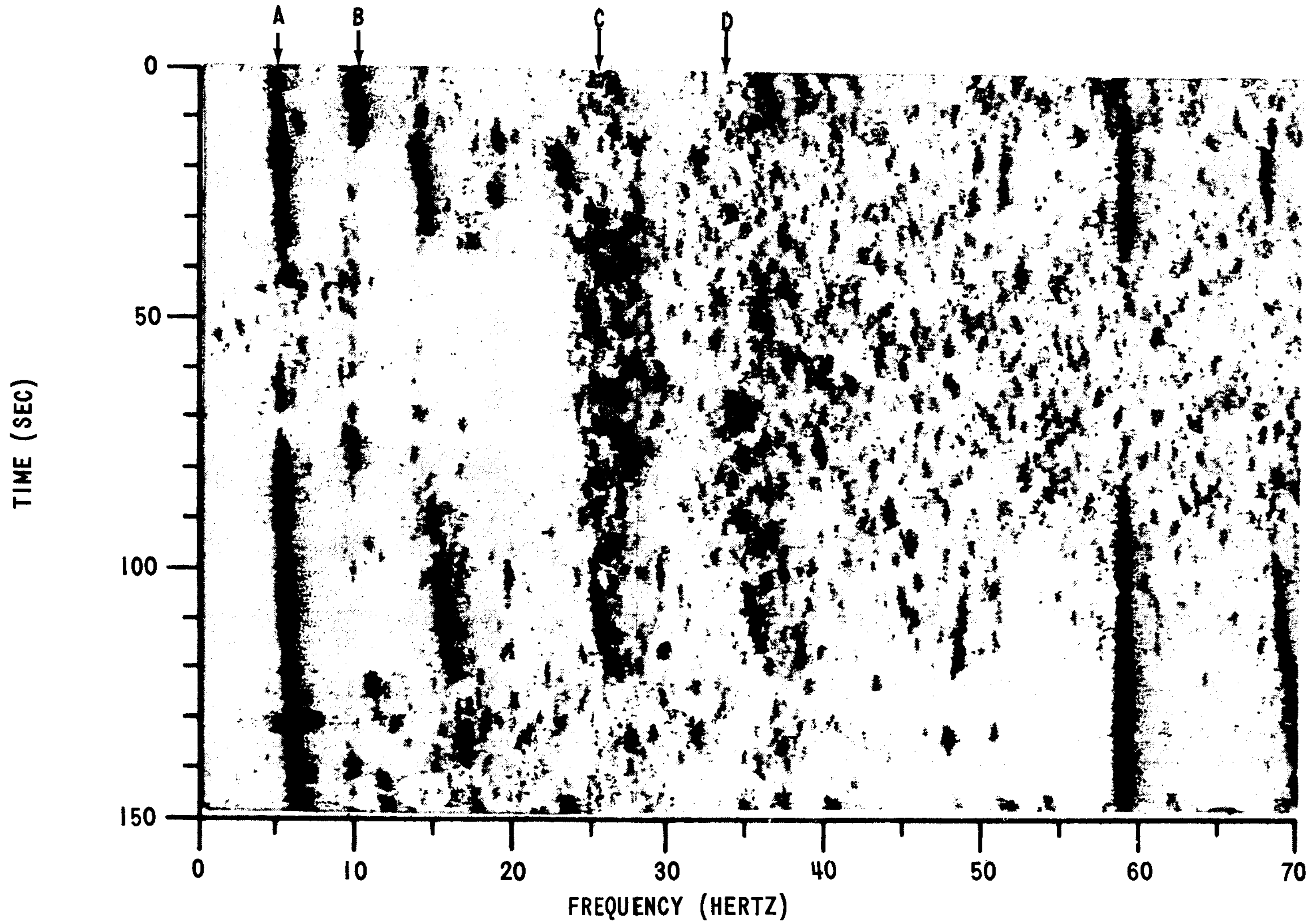

MEASUREMENT CK 0038A AS-501 AXIAL ACCELERATION - CM SWAY BRACE

FIGURE 14

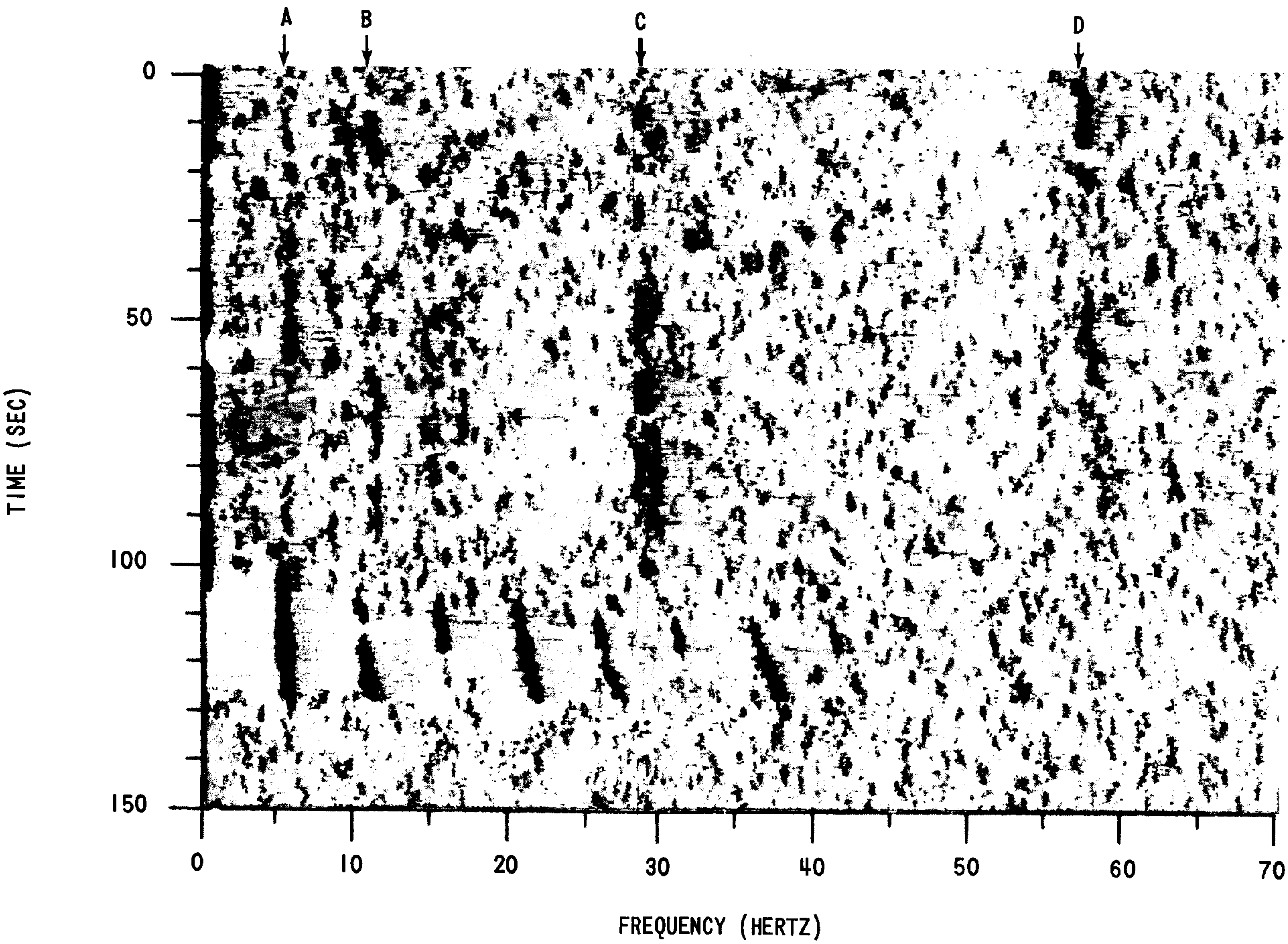

MEASUREMENT GA 7023A AS-502 Y AXIS ACCELERATION - LTA-2R

FIGURE 15

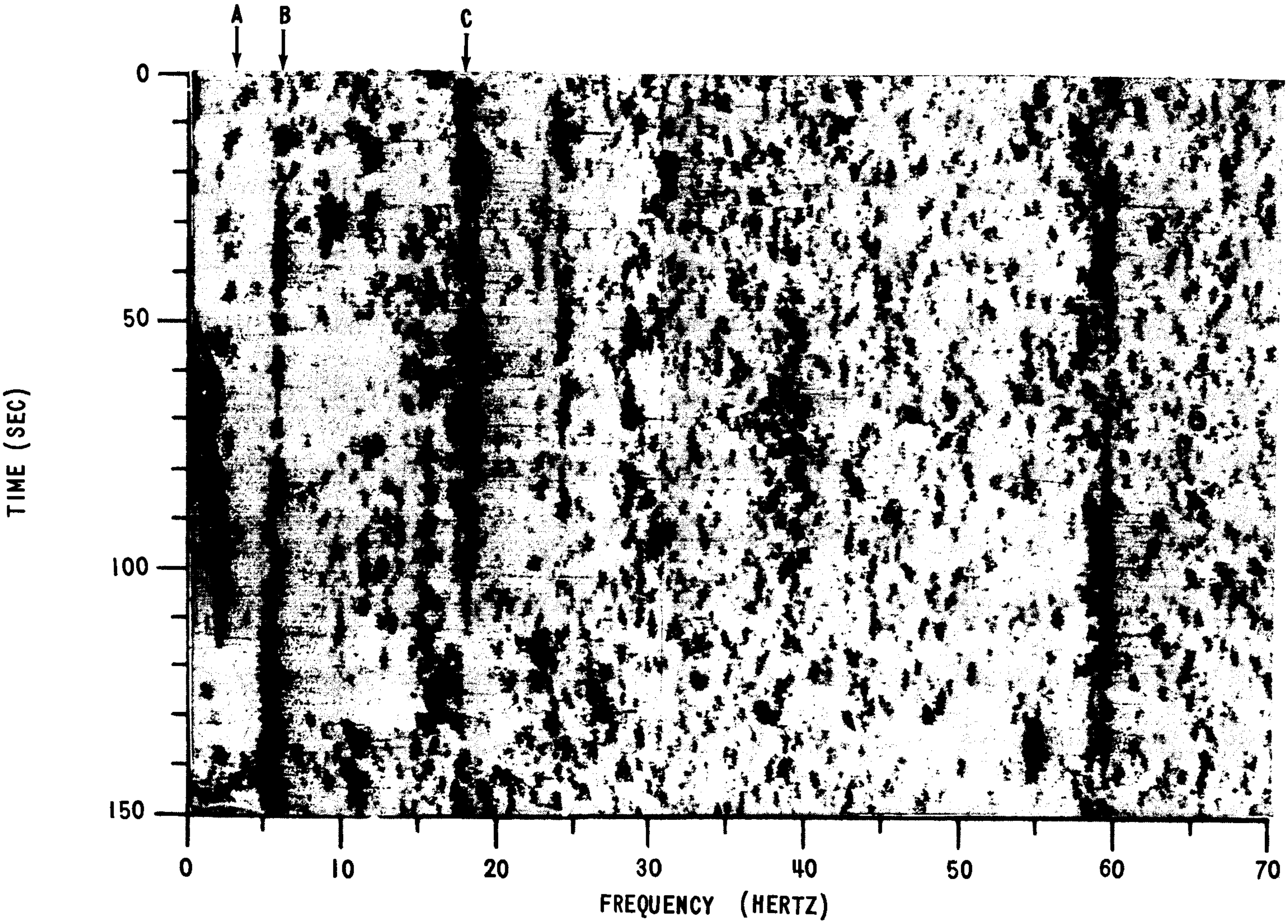

MEASUREMENT GA 7025A AS-502 Z AXIS ACCELERATION - LTA-2R

FIGURE 16

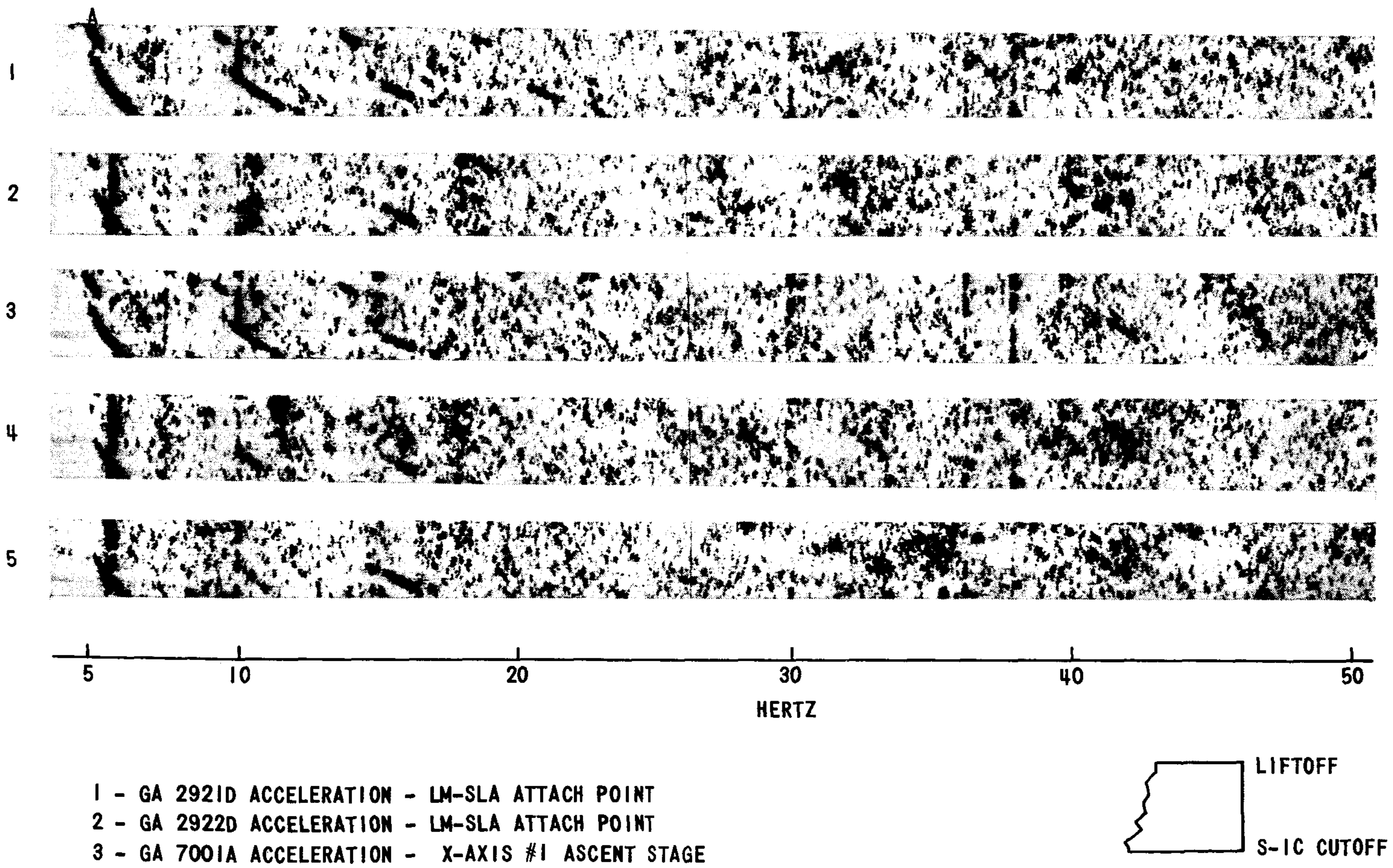

1 - GA 2921D ACCELERATION - LM-SLA ATTACH POINT
2 - GA 2922D ACCELERATION - LM-SLA ATTACH POINT
3 - GA 7001A ACCELERATION - X-AXIS #1 ASCENT STAGE
4 - GA 7003A ACCELERATION - Y-AXIS #1 ASCENT STAGE
5 - GA 7005A ACCELERATION - Z-AXIS #1 ASCENT STAGE

SPECTRUM ANALYSES - LTA-10R (AS-501)

FIGURE 17

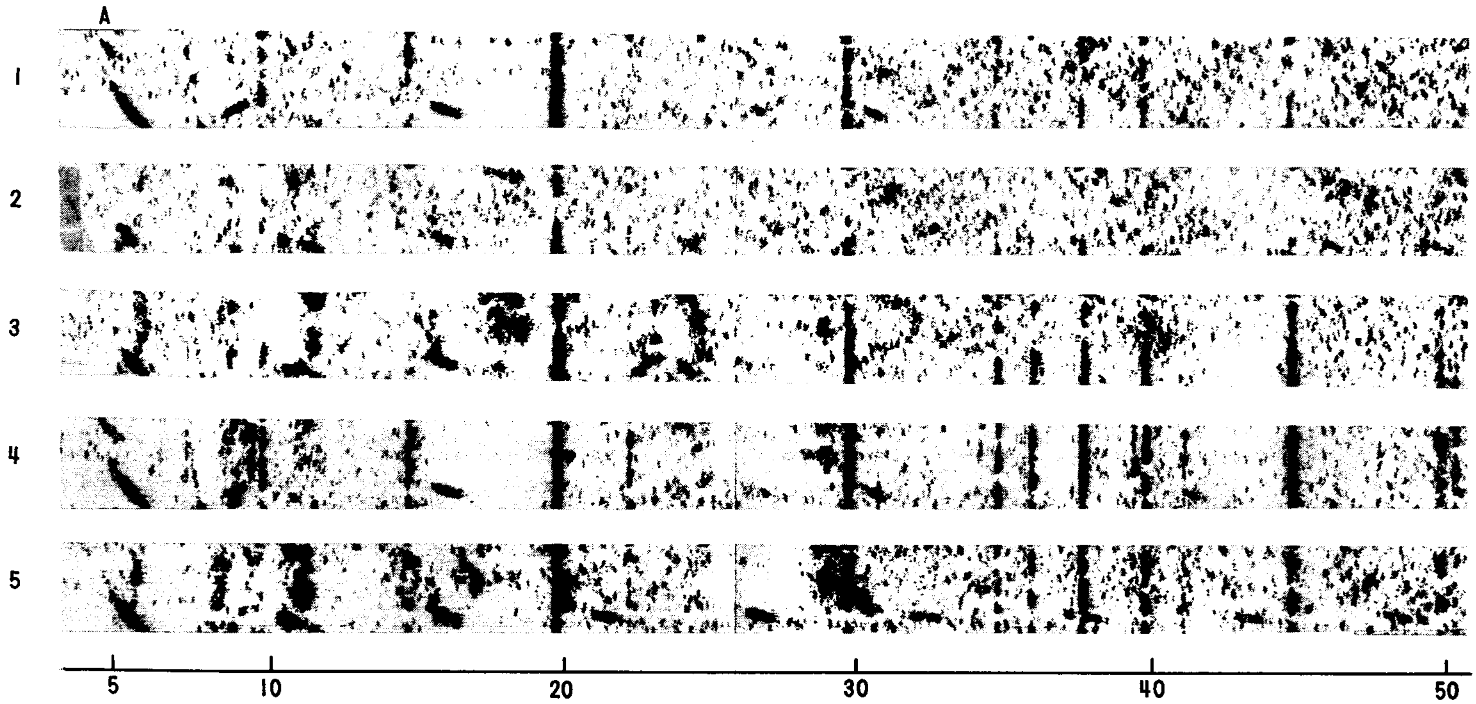

1 - GA 2921D ACCELERATION - LM-SLA ATTACH POINT
2 - GA 2922D ACCELERATION - LM-SLA ATTACH POINT
3 - GA 7011 ACCELERATION - X-AXIS #1 ASCENT STAGE
4 - GA 7013 ACCELERATION - Y-AXIS #1 ASCENT STAGE
5 - GA 7015 ACCELERATION - Z-AXIS #1 ASCENT STAGE

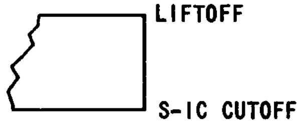

SPECTRUM ANALYSES - LTA-2R (AS-502)

FIGURE 18

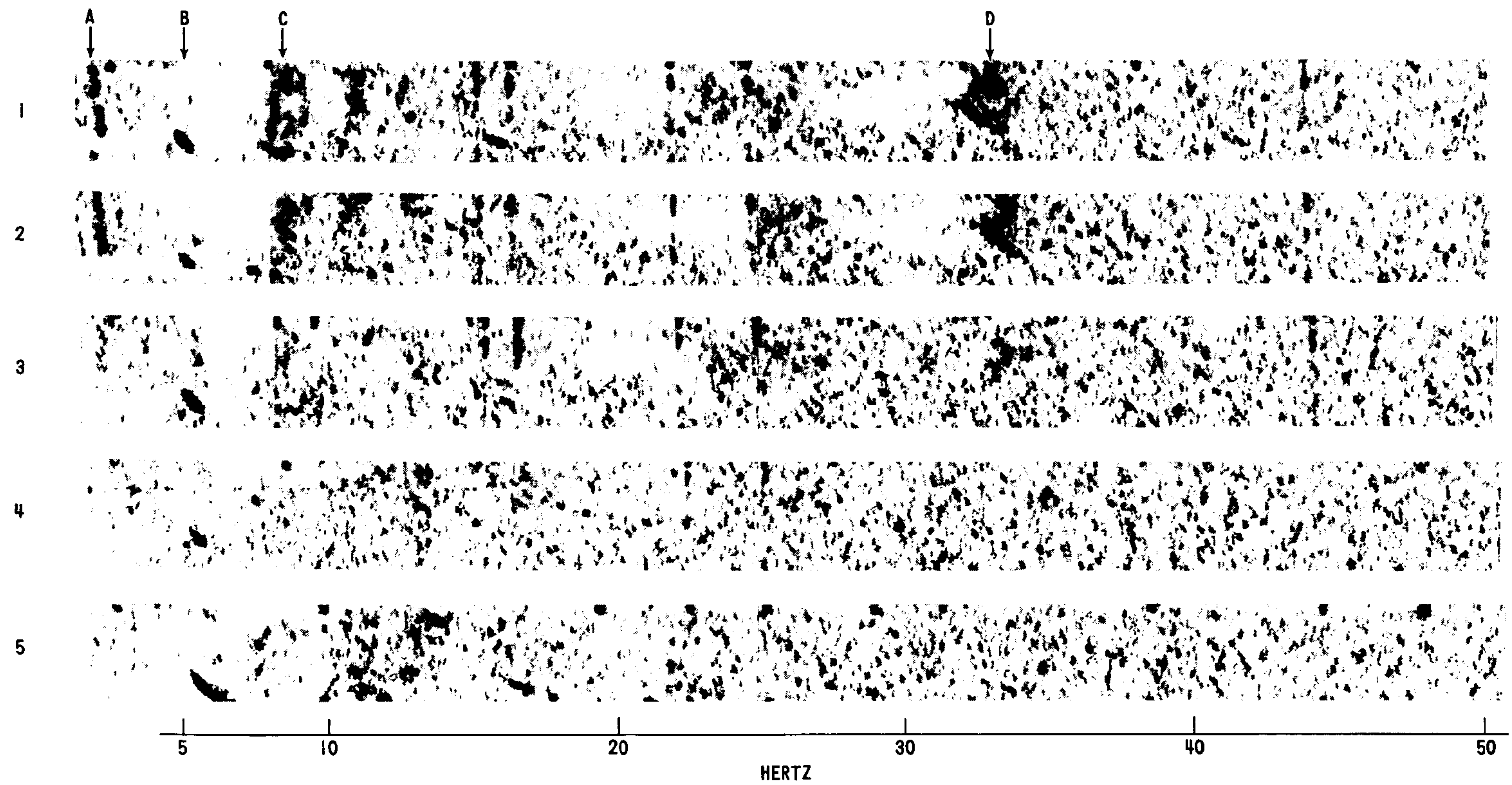

1 - Z-AXIS TOWER ACCELERATION LA 0012A
2 - Y-AXIS TOWER ACCELERATION LA 0011A
3 - Z-AXIS SPACECRAFT ACCELERATION CA 0007A
4 - TANGENTIAL ACCELERATION CM SWAY BRACE CK 0036A
5 - TANGENTIAL ACCELERATION CM SWAY BRACE CK 0037A

502 SPACECRAFT ACCELERATION

FIGURE 19

BELLCOMM, INC.

Subject: Spectrum Analysis of Apollo 4 and Apollo 6 Data - Case 320

From: J. Z. Menard

Distribution List

NASA Headquarters

L. E. Day - MAT
G. H. Hage - MA-A
R. S. Levine - RPL
S. C. Phillips - MA
W. E. Stoney, Jr. - MA

Langley Research Center

G. W. Brooks - 242

Manned Spacecraft Center

D. D. Arabian - PT4
C. H. Bolender - PA
J. A. Chamberlin - EA2
A. Cohen - PD
R. A. Colonna - PD5
M. A. Faget - EA
R. A. Gardiner - EG
P. C. Glynn - ES
G. E. Griffith - ES2
K. S. Kleinknecht - PA
J. N. Kotanchik - ES
J. B. Lee - EA2
G. M. Low - PA
O. E. Maynard - PD
C. T. Modlin - ES2
R. S. Sawyer - EE
J. R. Thibodeau - FM8
P. Vavra - EB
D. C. Wade - ES2

Marshall Space Flight Center

J. B. Bramlett - I-V-MGR-O
J. H. Farrow - R-P&VE-SV
E. E. Goerner - R-P&VE-A
W. A. Horn - R-P&VE-PPA
T. P. Isbell - R-P&VE-P
L. B. James - I-V-MGR
J. P. Lindberg, Jr. - R-AERO-F
W. R. Lucas - R-P&VE-DIR
H. R. Palaoro - R-P&VE-DIR
L. G. Richard - R-SE-DIR
N. Showers - R-P&VE-SL
J. B. Sterrett, Jr. - R-P&VE-S

Bellcomm

C. F. Banick
C. Bidgood
A. P. Boysen, Jr.
W. O. Campbell
D. A. Chisholm
L. A. Ferrara
D. R. Hagner
H. A. Helm
J. J. Hibbert
B. T. Howard
J. E. Johnson
P. F. Long
L. D. Nelson
J. M. Nervik
J. T. Raleigh
G. C. Reis
I. M. Ross
R. V. Sperry
J. W. Timko
G. B. Troussoff
R. L. Wagner
All members, Dept. 2031
Dept. 1024 File
Central File
Library